Applied Numerical Mathematics 174 (2022) 71–88

Contents lists available at ScienceDirect

Applied Numerical Mathematics

www.elsevier.com/locate/apnum

On numerical solution of Fredholm and Hammerstein integral equations via Nyström method and Gaussian quadrature rules for splines

D. Barrera [a,b,*], M. Bartoň [c,d], I. Chiarella [e], S. Remogna [e]

[a] Department of Applied Mathematics, University of Granada, Campus de Fuentenueva, 18071 Granada, Spain
[b] IMAG – Institute of Mathematics, Ventanilla 11, 18001 Granada, Spain
[c] Basque Center for Applied Mathematics, Alameda Mazarredo 14, 48009 Bilbao, Basque Country, Spain
[d] Iberbasque – Basque Foundation for Sciences, María Díaz de Haro 3, 48013 Bilbao, Basque Country, Spain
[e] Department of Mathematics "Giuseppe Peano", University of Torino, Via Carlo Alberto 10, 10123 Torino, Italy

ARTICLE INFO

Article history:
Received 8 August 2021
Received in revised form 3 November 2021
Accepted 13 January 2022
Available online 19 January 2022

Keywords:
Fredholm integral equation
Hammerstein integral equation
Nyström method
Numerical integration
Gaussian quadrature rules for splines

ABSTRACT

Nyström method is a standard numerical technique to solve Fredholm integral equations of the second kind where the integration of the kernel is approximated using a quadrature formula. Traditionally, the quadrature rule used is the classical polynomial Gauss quadrature. Motivated by the observation that a given function can be better approximated by a spline function of a lower degree than a single polynomial piece of a higher degree, in this work, we investigate the use of Gaussian rules for splines in the Nyström method. We show that, for continuous kernels, the approximate solution of linear Fredholm integral equations computed using spline Gaussian quadrature rules converges to the exact solution for $m \to \infty$, m being the number of quadrature points. Our numerical results also show that, when fixing the same number of quadrature points, the approximation is more accurate using spline Gaussian rules than using the classical polynomial Gauss rules. We also investigate the non-linear case, considering Hammerstein integral equations, and present some numerical tests.

1. Introduction

It is well-known that a quadrature rule (QR for short) to estimate the value of $I(f) := \int_a^b f(x)\,dx$ of a given function f defined on the interval $[a, b]$ is defined as

$$Q_m(f) := \sum_{i=1}^{m} \omega_i f(\tau_i), \tag{1.1}$$

where the coefficients $\omega_i := \omega_{i,m}$ and the pairwise distinct abscissae $\tau_i := \tau_{i,m}$, $1 \le i \le m$, are said to be the *weights* and the *nodes* of the rule, respectively. The QR given by (1.1) that requires m function evaluations are referred to as an m-point rule.

* Corresponding author at: Department of Applied Mathematics, University of Granada, Campus de Fuentenueva, 18071 Granada, Spain
E-mail address: dbarrera@ugr.es (D. Barrera).

https://doi.org/10.1016/j.apnum.2022.01.009

Usually, the remainder term

$$R_m(f) := I(f) - Q_m(f)$$

is required to be zero for each element of a predefined linear function space $\mathcal{L}$. In such a case the rule is said to be exact on $\mathcal{L}$. The rule (1.1) is said to be *Gaussian* if m is the minimal number of nodes at which f is evaluated and $R_m(f) = 0$ for all $f \in \mathcal{L}$. That is, Gaussian quadratures are optimal in terms of the number of quadrature points used. In the case when $\mathcal{L}$ is the linear space $\mathbb{P}_{2m-1}$ of polynomials of degree at most $2m-1$, then the classical Gaussian m-point QR is both exact and optimal in terms of the number of quadrature points. The nodes and the abscissae are computed using the orthogonal polynomials with respect to the measure dx or using the recursion algorithm of Golub and Welsch [15].

Classical techniques for numerically solving Fredholm integral equations of the second kind are Galerkin, collocation, Nyström and degenerate kernel methods (see the monograph [3]). Moreover, recently, spline quasi-interpolation has been shown to be very useful for this purpose (see e.g. [4,5,10,11]). Even though there are various alternative methods to solve Volterra and/or Fredholm integral equations, see e.g. [20–23] and other references cited therein, the Nyström method is a very efficient method to deal with integral equations. This method is based on the use of numerical integration, and typically Gaussian quadrature [14] or rules derived from spline quasi-interpolants are used. It is therefore quite natural to think of using Gaussian QR for spline spaces.

The topic of Gaussian quadratures for splines has been considered in [18,19], where the minimal number of nodes for the knot sequence associated with the spline space is derived, as well as the subintervals that must contain at least one node. The difficulty with spline Gaussian rules stems from the fact that the number of quadrature points in each knot span may vary depending on a particular knot vector. A numerical approach to compute the Gaussian spline rules, including spaces over non-uniform knot vectors, has been proposed recently [6].

In this paper, we both exploit the Gaussian spline rules derived recently [1,6,9] and the newly computed Gaussian quadrature rules for C^4 quintic splines over uniform knots to show that these rules act favorably in the Nyström method when compared to the classical polynomial Gauss rules. In particular, we show that when fixing the number of quadrature points, the Nyström method produces the smallest error when spline Gaussian rules are used. The closest work to ours is [25], where some spline Gaussian rules are used in the Nyström method to numerically solve Fredholm integral equations of the second kind. However, only spline spaces with maximum continuity are considered and the quadrature rules come from the solution of the non-linear systems of equations yielding the exactness of the rule for the functions in a basis of truncated powers. Our work extends [25] by studying the convergence rate, moreover, we compare Gaussian quadratures of spline spaces of various continuities and apply them also to non-linear integral equations. The rest of the paper is organized as follows. Section 2 concerns spline Gaussian QR for certain spline spaces. Then we describe the Nyström method in Section 3 and present numerical results in Section 4 for linear integral equations. In Section 5 we also investigate the non-linear case, considering Hammerstein integral equations and propose some numerical tests. Finally, we conclude the paper in Section 6.

2. Gaussian quadrature for splines

In this section, we recall the main results related to spline spaces [13] and we propose the Gaussian rules for splines for the numerical evaluation of $I(f)$.

2.1. Spline spaces

We consider the break points $\mathbf{x} := \{x_i\}_{i=0}^{n}$ such that $a = x_0 < x_1 < \ldots < x_{n-1} < x_n = b$ and the space $\mathbb{P}_{p,\mathbf{x}}$ of piecewise polynomial functions of degree p (and order $d = p+1$) associated with the partition of $[a,b]$ induced by $\mathbf{x}$. Let $\mathbf{r} := \{r_i\}_{i=1}^{n-1}$ be a vector with entries $r_i \le d$, and consider the subspace $\mathbb{P}_{p,\mathbf{x},\mathbf{r}}$ formed by all functions in $\mathbb{P}_{p,\mathbf{x}}$ of C^{r_i-1} class at x_i, $1 \le i \le n-1$. Its dimension is equal to

$$N := dn - \sum_{i=1}^{n-1} r_i. \tag{2.1}$$

Let $\mathbf{u} := \{u_i\}_{i=1}^{N+d}$ be the knot sequence formed by the break points x_i repeated $d - r_i$ times, $u_1 \le u_2 \le \ldots \le u_d \le x_0$ and $x_n \le u_{N+1} \le u_{N+2} \le \ldots \le u_{N+d}$. The integer $d - r_i$ denotes the *knot multiplicity* and $r_i - 1$ is the spline *regularity* at x_i. We further define the k-th normalized B-spline of degree p and order d as

$$B_{k,p}(x) := \left(u_{k+p+1} - u_k\right)\left[u_k, \ldots, u_{k+p+1}\right](\cdot - x)_+^p, \quad x \in \mathbb{R},$$

where $\left[z_0, \cdots, z_{p+1}\right] f$ stands for the divided difference at knots $z_0, \ldots, z_{p+1}$ for the function f, and $z_+ := \max(0, z)$ denotes the truncated power. The B-spline $B_{k,p}$ is a piecewise polynomial function of degree p, supported on $\left[u_k, u_{k+p+1}\right]$ and positive on $\left(u_k, u_{k+p+1}\right)$. The B-splines $B_{k,p}$ can be computed by using the de Boor-Cox recurrence formula

$$B_{k,0}(x) = \begin{cases} 1, & \text{if } x \in [u_k, u_{k+1}), \\ 0, & \text{otherwise,} \end{cases}$$

$$B_{k,p}(x) = \frac{x - u_k}{u_{k+p} - u_k} B_{k,p-1}(x) + \frac{u_{k+p+1} - x}{u_{k+p+1} - u_{k+1}} B_{k+1,p}(x), \quad p > 0,$$

where by convention the value 0 is assigned when the term 0/0 appears. By Curry-Schoenberg's Theorem [13], we know that the sequence $\{B_{k,p}\}_{k=1}^{N}$ is a basis of $\mathbb{P}_{p,\mathbf{x},\mathbf{r}}$, and it holds

$$S_p^n = \operatorname{span}\left\{B_{k,p}(u), u \in [u_d, u_{N+1}]\right\} = \mathbb{P}_{p,\mathbf{x},\mathbf{r}}.$$

Another normalization can be used to define the Curry-Schoenberg's B-spline as follows:

$$M_{k,p}(x) := \frac{p+1}{u_{k+p+1} - u_k} B_{k,p}(x), \quad x \in \mathbb{R}.$$

Therefore, we have

$$M_{k,p}(x) = (p+1)\left[u_k, \ldots, u_{k+p+1}\right](\cdot - x)_+^p,$$

and taking into account that

$$\left[u_k, \ldots, u_{k+p+1}\right] f = \frac{1}{p!} \int_a^b \frac{M_{k,p}(x)}{p+1} D^{p+1} f(x)\, dx,$$

it follows that $\frac{M_{k,p}}{p+1}$ is the Peano kernel of the linear functional $\left[u_k, \ldots, u_{k+p+1}\right]$ when applied to $f \in C^{p+1}([a,b])$ with $u_k, \ldots, u_{k+p+1} \in [a,b]$. As a consequence,

$$\int_a^b M_{k,p}(x)\, dx = 1.$$

However, the QRs in the following subsection use the *non-normalized* B-spline defined as

$$D_{k,p}(x) := \frac{1}{p+1} M_{k,p}(x) = \left[u_k, \ldots, u_{k+p+1}\right](\cdot - x)_+^p, \ x \in \mathbb{R} \tag{2.2}$$

and the two definitions of a basis function are linked via the following relation:

$$\int_a^b D_{k,p}(x)\, dx = \frac{1}{p+1} \int_a^b M_{k,p}(x)\, dx = \frac{1}{p+1}.$$

In the subsequent sections, where the used degree is clear, we omit it. In the case of uniform regularity, i.e. $r_i = \mu + 1$, $1 \le i \le n-1$ the following notation will be used:

$$S_{p,\mu}^n = \left\{f \in C^{\mu}([a,b]) : f_{|[x_i, x_{i+1}]} \in \mathbb{P}_p, \ i = 0, \ldots, n-1\right\},$$

where $\mathbb{P}_p$ denotes the space of polynomials of degree p. The existence of Gaussian QRs for these spaces with uniform regularity is proved in [17] and the uniqueness in [19, Theorem 3.4]. Moreover, the following relationship holds:

$$p + \ell + 1 = 2m,$$

where p is the polynomial degree, ℓ the total number of interior knots (when counting multiplicities), and m is the number of Gaussian nodes. This fact is in accordance with the dimension count of the spline space, cf. Eq. (2.1), that is $N = p + \ell + 1$, which is the maximum number of basis functions that is expected to be integrated exactly by only half the number of quadrature points. If p is assumed to be small compared to ℓ, then the number of quadrature points is approximately half the number of interior knots in the integration interval. In the limit, when $n \to \infty$, the spline rules converge to the half-point rules of Hughes et al. [16], that are exact and optimal over the whole real line.

2.2. Quadrature rules for C^1 cubic splines with uniform knots

In general, Gaussian rules for splines cannot be computed analytically, however, for certain specific spaces, e.g. of lower degrees over special knot vectors, one can compute the weights and nodes in a closed form fashion using a recursive formula [1,9,24]. One such a prominent spline space is C^1 cubic splines with uniform knots, which has the special structure that guarantees existence of a single quadrature point in every element, except the middle one that requires two [24]. This fact allows us to construct a recursive algorithm that starts in the boundary element, computes the first node and weight analytically, and proceeds towards the middle of the domain, computing the following nodes and weights using a recursive formula containing the nodes and weights from the preceding element. Let consider $[a,b]=[0,1]$ and fix in $[0,1]$ the break points $\mathbf{x}:=\{x_i\}_{i=0}^{n}$ with $x_i:=\frac{i}{n}$, $\mathbf{r}:=\{r_i\}_{i=1}^{n-1}$ with $r_i=2$ and define

$$S_{3,1}^{n}:=\left\{f\in C^1([0,1]):f_{|[x_r,x_{r+1}]}\in\mathbb{P}_3,\ r=0,1,\ldots,n-1\right\}.$$

For this space over n uniform elements, the main goal is to look for the Gaussian QR that is known to need only $m=n+1$ quadrature points, that is

$$Q_{n+1}(f)=\sum_{i=1}^{n+1}\omega_i f(\tau_i),\quad 0<\tau_1<\ldots<\tau_{n+1}<1. \tag{2.3}$$

Since there exists only one optimal rule, it must be symmetrical, so it is sufficient to determine the left half of the nodes and weights. The next result is proved in [24, Theorem 2.1] and, depending on the parity of the elements n, it gives a recursive formula to compute the nodes and weights.

Theorem 1. *Let $\omega_i=\frac{\delta_i}{n}$ and $\tau_i=\frac{(i-\theta_i)}{n}$, $i=1,\ldots,\lfloor n/2\rfloor+1$, be the weights and nodes of the m-point Gaussian QR (2.3), where $\lfloor z\rfloor$ stands for the integer part of z. Then, the sequences $(\delta_i)_{1\le i\le\lfloor n/2\rfloor+1}$ and $(\theta_i)_{1\le i\le\lfloor n/2\rfloor+1}$ are determined by*

$$\delta_1=\frac{16}{27},\quad \theta_1=\frac{3}{4},$$

and for, $i=1,\ldots,\lfloor n/2\rfloor-1$, by the recurrence relations

$$\theta_{i+1}=\frac{1-\delta_i(1-\theta_i)^2(5\theta_i+1)}{1-\delta_i(1-\theta_i)^2(4\theta_i+1)}\quad\text{and}\quad \delta_{i+1}=\frac{1-\delta_i(1-\theta_i)^2(4\theta_i+1)}{\theta_{i+1}^2}. \tag{2.4}$$

If n is even, say $n=2l$, then $\theta_{l+1}=1$ and

$$\delta_{l+1}=1-2\delta_l(1-\theta_l)^2\left(2\theta_{l+1}+1\right).$$

If n is odd, say $n=2l-1$, then

$$\delta_l=1-\delta_{l-1}\left(1-\theta_{l-1}\right)^2\left(2\theta_{l-1}+1\right)$$

and θ_l is the greater zero of the equation

$$\theta_l(1-\theta_l)=\frac{\delta_{l-1}\theta_{l-1}\left(1-\theta_{l-1}\right)^2}{1-\delta_{l-1}\left(1-\theta_{l-1}^2\right)\left(2\theta_{l-1}+1\right)}.$$

Note that the δ- and θ-sequences do not depend on n, and (considered as infinite sequences, defined by (2.4)) both tend monotonically to 1 with second-order convergence. Theorem 1 constructs the QR on the unit interval. For non-unit intervals, the quadrature is mapped via an affine transformation. That is, for a general interval $[a,b]$ we get $\bar{w}_i:=(b-a)\,\omega_i$, and $\bar{\tau}_i:=(b-a)\,\tau_i+a$, where ω_i and τ_i are the weights and the nodes computed on the unit interval.

For $f\in C^4([0,1])\setminus S_{3,1}^{n}$, then there exists $z\in[0,1]$ such that

$$R_{n+1}(f)=I(f)-Q_{n+1}(f)=c_{n+1,4}f^{(4)}(z),$$

where [24, Theorem 2.2, eq. (2.6)]

$$c_{n+1,4}=\frac{1}{720n^4}-\frac{1}{12}\sum_{i=1}^{\left\lfloor\frac{n+1}{2}\right\rfloor}\omega_i\left(x_{i-1}-\tau_i\right)^2\left(x_i-\tau_i\right)^2.$$

Moreover, from [24, Corollary 2.3] it holds

$$\frac{1}{720n^4}-\frac{1}{551.9775n^5}\leq c_{n+1,4}\leq\frac{1}{720n^4}-\frac{1}{552n^5}.$$

The proof of Theorem 1 is based on the representation of the spline functions in $S^n_{3,1}$ in terms of the basis of B-splines $D_{k,3}$ in (2.2). Let $x_{-1}:=-\frac{1}{n}$ and $x_{n+1}:=1+\frac{1}{n}$ be two extra break points, added to the partition $\mathbf{x}$ of the interval $[0,1]$ in order to obtain the extended knot partition $\mathbf{u}:=\{u_i\}_{i=1}^{N+4}$, with $N=2n+2$ and $u_{2i+3}=u_{2i+4}=x_i$, $i=-1,\ldots,n+1$. Therefore, the B-splines are given explicitly by the following expressions: for $r=1,\ldots,n+1$,

$$\begin{aligned}D_{2r-1}(t)&=[x_{r-2},x_{r-2},x_{r-1},x_{r-1},x_r](\cdot-t)_+^3,\\ D_{2r}(t)&=[x_{r-2},x_{r-1},x_{r-1},x_r,x_r](\cdot-t)_+^3.\end{aligned}\tag{2.5}$$

They are supported on $[x_{r-2},x_r]$ and positive on (x_{r-2},x_r).

2.3. Quadrature rules for C^1 quintic splines with uniform knots

Another spline space that admits to compute the Gaussian QR using a recursive formula is C^1 quintic splines with uniform knots. For this space, each element is guaranteed to have two Gaussian points, except the middle one that requires three [9]. Analogously to [24], the nodes and weights can be computed analytically using a recursive formula. The construction of QRs for C^1 quintic splines with uniform knots proceeds as follows, see also [9]. For a given set of break points $\mathbf{x}:=\{x_i\}_{i=0}^n$, $x_i:=a+(i-1)h$, $1\leq i\leq n+1$, with steplength $h:=(b-a)/n$, and $\mathbf{r}:=\{r_i\}_{i=1}^{n-1}$ with $r_i=2$, the spline space considered is

$$S^n_{5,1}:=\left\{f\in C^1([a,b]):f_{|[x_r,x_{r+1}]}\in\mathbb{P}_5,\ r=0,1,\ldots,n-1\right\}.$$

Its dimension is equal to $\dim S^n_{5,1}=(5+1)+4(n-1)=4n+2$, therefore the number of nodes of the Gaussian QR is equal to $2n+1$.

As in the C^1 cubic case, in order to derive a recurrence method to determine the weights and nodes, an appropriate basis to $S^n_{5,1}$ is considered, whose non-normalized B-splines are defined by (2.2). Therefore, an appropriate extended partition $\mathbf{u}$ is needed. It is achieved from $\mathbf{x}$ and $\mathbf{r}$, by adding two additional break points $x_{-1}:=a-h$ and $x_{n+1}:=b+h$ with multiplicity two. It is given by $\mathbf{u}:=\{u_i\}_{i=1}^{N+6}$, with $N=4n+2$ and $u_{4i+3}=u_{4i+4}=u_{4i+5}=u_{4i+6}=x_i$, $i=0,\ldots,n$, and $u_1=u_2=x_{-1}$, $u_{4n+7}=u_{4n+8}=x_{n+1}$. From this partition the basis $\{D_i\}_1^{4n+2}$ is defined according (2.2) to obtain the following expressions:

$$\begin{aligned}D_{4k-3}(t)&=[x_{k-2},x_{k-2},x_{k-1},x_{k-1},x_{k-1},x_{k-1},x_k](\cdot-t)_+^5,\\ D_{4k-2}(t)&=[x_{k-2},x_{k-1},x_{k-1},x_{k-1},x_{k-1},x_k,x_k](\cdot-t)_+^5,\quad k=1,\ldots,n+1,\\ D_{4k-1}(t)&=[x_{k-1},x_{k-1},x_{k-1},x_{k-1},x_k,x_k,x_k](\cdot-t)_+^5,\\ D_{4k}(t)&=[x_{k-1},x_{k-1},x_{k-1},x_k,x_k,x_k,x_k](\cdot-t)_+^5,\quad k=1,\ldots,n.\end{aligned}$$

Functions D_{4k-3} and D_{4k-2} are supported on $[x_{k-2},x_k]$, while the supports of D_{4k-1} and D_{4k} are equal to $[x_{k-1},x_k]$, see Fig. 1. Moreover, after some computations, the following expressions are obtained: for $t\in[x_{k-2},x_k]$ it holds

$$\begin{aligned}D_{4k-3}(t)&=\frac{1}{4h^6}(t-x_{k-2})^4(x_k+8x_{k-1}-9t),\\ D_{4k-2}(t)&=\frac{1}{4h^6}(t-x_{k-2})^5,\end{aligned}$$

and for $t\in[x_{k-1},x_k]$ we have

$$\begin{aligned}D_{4k-3}(t)&=\frac{1}{4h^6}(x_k-t)^5,\\ D_{4k-2}(t)&=\frac{1}{4h^6}(x_k-t)^4(9t-8x_{k-1}-x_{k-2}),\\ D_{4k-1}(t)&=\frac{10}{h^6}(t-x_{k-1})^2(x_k-t)^3,\\ D_{4k}(t)&=\frac{10}{h^6}(t-x_{k-1})^3(x_k-t)^2.\end{aligned}\tag{2.6}$$

For every interval $[x_{k-1},x_k]$ only six B-splines have supports intersecting it.

A detailed study in [9] leads to a recurrence method to determine the nodes and weights of the $(2n+1)$-Gaussian QR

$$Q_{2n+1}(f):=\sum_{i=1}^{2n+1}\omega_i f(\tau_i)\tag{2.7}$$

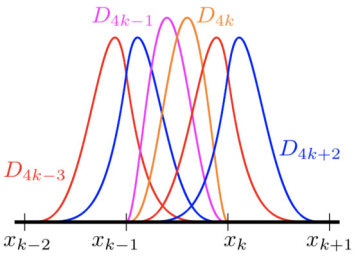

Fig. 1. Only the B-splines $D_{4k-3},\dots,D_{4k+2}$ have supports intersecting the interval $[x_{k-1},x_k]$.

to approximate $I(f)$. They are summarized in the following result (see Theorem 2.1 in [9]), that, similarly to Theorem 1, considers two scenarios depending on the parity of n.

Theorem 2. *Let $A_1 := \frac{1}{24}$ and $B_1 := \frac{1}{8}$, and for $k = 2,\dots,\lfloor n/2\rfloor + 1$ define*

$$A_k := I\left(D_{4k-3}\right) - \omega_{2k-3} D_{4k-3}\left(\tau_{2k-3}\right) - \omega_{2k-2} D_{4k-3}\left(\tau_{2k-2}\right),$$
$$B_k := I\left(D_{4k-2}\right) - \omega_{2k-3} D_{4k-2}\left(\tau_{2k-3}\right) - \omega_{2k-2} D_{4k-2}\left(\tau_{2k-2}\right).$$

Then, the nodes and weights relative to the Gaussian QR (2.7) are determined by recurrence as follows: for $k = 1,\dots,\lfloor n/2\rfloor$,

$$\tau_{2k-1} = x_{k-1} + \frac{-b_k - \sqrt{b_k^2 - 4a_k c_k}}{2a_k} \text{ and } \tau_{2k} = x_k - \frac{-b_k + \sqrt{b_k^2 - 4a_k c_k}}{2a_k},$$

with

$$a_k := 1 - 480A_k + 576A_k^2 + 576B_k^2 - 1152A_k B_k,$$
$$b_k := 2h\left(12B_k + 108A_k - 1\right),$$
$$c_k := h^2\left(1 - 24B_k + 24A_k\right),$$

and

$$\omega_{2k-1} = \frac{2h^5\left(9\beta_k A_k + hA_k - hB_k + \beta_k B_k\right)}{5\left(h - \tau_{2k-1} + x_{k-1}\right)^4\left(\tau_{2k} - \tau_{2k-1}\right)},$$
$$\omega_{2k} = \frac{h^5\left(2\tau_{2k-1} - 2x_{k-1} - h\right)}{60\left(\tau_{2k} - x_{k-1}\right)^2\left(h - \tau_{2k} + x_{k-1}\right)^2\left(\tau_{2k-1} - \tau_{2k}\right)}.$$

If n is even, namely $n = 2l$, then

$$\tau_{n+1} = x_l = \frac{a+b}{2} \quad \text{and} \quad \omega_{n+1} = \frac{2}{3}h - \frac{2\alpha_l^2\left(5h - 4\alpha_l\right)\omega_{n-1} + 2\beta_l^4\left(5h - 4\beta_l\right)\omega_n}{h^5},$$

with $\alpha_l := \tau_{n-1} - x_{l-1}$ and $\beta_l := \tau_n - x_{l-1}$. If n is odd, namely $n = 2l-1$, then $\tau_{n+1} = \frac{a+b}{2}$,

$$\tau_n = x_{l-1} + \frac{-\tilde{b}_l - \sqrt{\tilde{b}_l^2 - 4\tilde{a}_l\tilde{c}_l}}{2\tilde{a}_l},$$

where

$$\widetilde{a}_l := 2\left(108A_l + 12B_l - 1\right),$$
$$\widetilde{b}_l := -2h\left(108A_l + 12B_l - 1\right),$$
$$\widetilde{c}_l := -h^2\left(24A_l - 24B_l + 1\right),$$

and τ_{n+2} is the symmetrical point of τ_n with respect to τ_{n+1}. Moreover, the associated weights are given by the expressions

$$\omega_n = \omega_{n+2} = \frac{h\left(108A_l + 12B_l - 1\right)^2}{30\left(156A_l - 36B_l + 1\right)},$$
$$\omega_{n+1} = \frac{4h\left(1152A_l B_l + 264A_l - 576A_l^2 - 576B_l^2 - 24B_l + 1\right)}{15\left(156A_l - 36B_l + 1\right)}.$$

It can be seen that the cost of integration with this method is reduced by 2/3 compared to the classical Gaussian quadrature for polynomials as the spline rule requires asymptotically (for large n) only two quadrature points per element while the polynomial Gauss needs three. This cost reduction is even more significant in multivariate (tensor product) setups where this "cost saving ratio" 2/3 powers by the dimension.

The rule from Theorem 2 is guaranteed to exactly integrate C^1 quintic splines. One can use the rule also for quintic spaces of higher continuities over uniform knot vectors (as these spaces are contained), however, the rule is not optimal in terms of number of quadrature points anymore.

For functions outside the spline space of interest, the integration error can be estimated using [9, Theorem 3.1]. That is, for $f \in C^6([a,b]) \setminus S^n_{5,1}$ there exists $\xi \in [a,b]$ such that

$$R_{n+1}(f) = I(f) - Q_{n+1}(f) = c_{2n+1,6} f^{(6)}(\xi),$$

where

$$c_{2n+1,6} = \frac{(b-a)^7}{5040} - \frac{1}{720} \sum_{k=1}^{2n+1} \omega_k (\tau_k - a)^6.$$

2.4. Quadrature rules for C^2 cubic and C^4 quintic splines by homotopy continuation

While for C^1 cubic and quintic spline spaces there exist recursive formulas to compute Gaussian QRs, for higher continuities such explicit formulas are not at hand. To this end, one has to derive the QRs numerically. Polynomial homotopy continuation (PHC) is a numerical scheme that solves polynomial systems of equations (for a detailed explanation, see the book [27]) and it has been used in [6–8] for generating Gaussian quadrature rules for splines. In particular, to generate a Gaussian quadrature rule in a given (target) spline space, an associated source space with known Gaussian quadrature is built and the rule from the source space to the target space is transferred, while preserving the number of quadrature points and therefore optimality. The exactness of the quadrature rule is formulated as a polynomial system and the quadrature nodes and weights, considered as a higher-dimensional point, are a zero of this system. Using the homotopy continuation concept, the source space is continuously deformed by changing the source knot vector to the target configuration and the quadrature rule gets updated numerically by tracing the unique root of the continuously modified (piecewise polynomial) system.

We consider a uniform knot vector $\mathbf{x}$ on the interval $[a,b]$ as in Section 2.2, where each of the $n-1$ interior knots has associated multiplicity two and the spline space $S^n_{3,1}$. We define $h := \frac{b-a}{n} = x_r - x_{r-1}$ for all $r = 1, \dots, n$. Let us denote $\tilde{n} := 2n-1$ and consider a uniform knot vector

$$\tilde{\mathbf{x}} = (a = \tilde{x}_0, \tilde{x}_1, ..., \tilde{x}_{\tilde{n}-1}, \tilde{x}_{\tilde{n}} = b)$$

such that each its knot is of multiplicity one. Then the spline space is

$$S^{\tilde{n}}_{3,2} = \{ f \in C^2([a,b]) : f_{|[\tilde{x}_{k-1}, \tilde{x}_k]} \in \mathbb{P}_3, \quad k = 1, \dots, \tilde{n} \}$$

and we further define $\tilde{h} := \frac{b-a}{\tilde{n}} = \tilde{x}_r - \tilde{x}_{r-1}$ for all $r = 1, \dots, \tilde{n}$. The dimension of both spaces is $2n+2$, that is, the total number of interior knots is the same for both spaces, while the number of non-zero knot spans is different.

Moreover, we consider the two extended partitions $\mathbf{u}$, obtained by considering x_0 and x_n as double knots and adding two extra double knots outside the interval $[a,b]$ that we set as to be

$$x_{-1} = x_0 - h \qquad \text{and} \qquad x_{n+1} = x_n + h, \tag{2.8}$$

and $\tilde{\mathbf{u}}$, obtained by extending the knot sequence of $\tilde{\mathbf{x}}$ by two triplets of single knots as

$$\tilde{x}_{-k} = \tilde{x}_0 - k\tilde{h} \qquad \text{and} \qquad \tilde{x}_{\tilde{n}+k} = \tilde{x}_{\tilde{n}} + k\tilde{h}, k = 1, 2, 3. \tag{2.9}$$

We define $\{\tilde{D}_k\}_{k=1}^{2n+2}$ the basis of the target space $S^{\tilde{n}}_{3,2}$ where

$$\tilde{D}_k(t) = [\tilde{x}_{k-4}, \dots, \tilde{x}_k](\cdot - t)^3_+, \quad k = 1, \dots, 2n+2.$$

We further have that

$$I(\tilde{D}_k) = I(D_k), \qquad k = 4, \dots, 2n-1, \tag{2.10}$$

where $\{D_k\}_{k=1}^{2n+2}$ is the basis of the source space $S^n_{3,1}$, defined as in (2.5). The ten boundary integrals (five only due to symmetry) are computed directly by integrating the corresponding B-splines. These integrals change during continuation and therefore have to be recomputed for various continuation parameter t, typically $t \in [0,1]$; $t = 0$ (source), $t = 1$ (target).

Now we consider a continuous transition between the source $S^n_{3,1}$ and target $S^{\tilde{n}}_{3,2}$. Since the transition of the spline spaces is governed by the transformation of the corresponding knot vectors, we consider the mapping

$$\mathbf{x} \to \tilde{\mathbf{x}}$$

including the six outer knots defined in (2.8) and (2.9). Due to the fact that we work with non-normalized basis functions, (2.10) remain unchanged. The total number of knots is $2n+6$, but since the two boundary knots are constrained to stay fixed, there are $2n+4$ free knots. The transformation can be conceptualized as a curve between $\mathbf{x}$ and $\tilde{\mathbf{x}}$, two points in $\mathbb{R}^{2n+4}$. There exist infinitely many paths connecting the source and target knot vectors. In particular, we use the geodesic path when considering the Euclidean metric on the vector of free knots.

We set our source space as $S^n_{3,1}$ for which we know a Gaussian source quadrature rule of the form (2.3), with nodes and weights given in Theorem 1. Due to the equal dimensions of $S^n_{3,1}$ and $S^{\tilde{n}}_{3,2}$, the target rule requires the same number of nodes and therefore we look for a QR of the form

$$\tilde{Q}_{n+1}(f) = \sum_{i=1}^{n+1} \tilde{\omega}_i f(\tilde{\tau}_i).$$

During the continuation, we transform the spline space $S^n_{3,1}$ to $S^{\tilde{n}}_{3,2}$ and accordingly the Gaussian rule $Q_{n+1} \to \tilde{Q}_{n+1}$. Therefore $\tilde{Q}_{n+1}$, represented by its nodes and weights, is a function of t. Without loss of generality, we conceptualize $t=0$ (source) and $t=1$ (target) and write the source quadrature rule as $Q_{n+1} = \tilde{Q}_{n+1}(0)$ and the target rule as $\tilde{Q}_{n+1} = \tilde{Q}_{n+1}(1)$. The vector of unknowns consisting of the quadrature nodes and weights is conceptualized as a $(2n+2)$-dimensional point

$$(\tilde{\tau}_1, \dots, \tilde{\tau}_{n+1}, \tilde{\omega}_1, \dots, \tilde{\omega}_{n+1}) \in \mathbb{R}^{2n+2}$$

and the source polynomial system expresses that exactness condition, i.e., that the source rule exactly integrates the source basis. The source root that solves it is the quadrature rule of Section 2.2. By using the homotopy framework, in [6] a Gaussian QR for uniform C^2 cubic spline spaces has been constructed, see [6] for more details.

By using the same logical argument, it is possible to derive a QR for uniform C^4 quintic spline spaces, starting from the QR of Section 2.3 for C^1 quintic splines with uniform knot sequences. In this case, we consider a uniform knot vector $\mathbf{x}$ on the interval $[a,b]$ as in Section 2.3, where each of the $n-1$ interior knots has associated multiplicity four. We denote the associated source spline space by $S^n_{5,1}$. We define $h := \frac{b-a}{n} = x_r - x_{r-1}$ for all $r = 1, \dots, n$. Let us denote $\tilde{n} := 4n-3$ and consider a uniform knot vector

$$\tilde{\mathbf{x}} = (a = \tilde{x}_0, \tilde{x}_1, \dots, \tilde{x}_{\tilde{n}-1}, \tilde{x}_{\tilde{n}} = b)$$

such that each its knot is of multiplicity one. Then the target spline space is

$$S^{\tilde{n}}_{5,4} = \{f \in C^4([a,b]) : f_{|[\tilde{x}_{k-1}, \tilde{x}_k]} \in \mathbb{P}_5, \quad k = 1, \dots, \tilde{n}\}$$

and we further define $\tilde{h} := \frac{b-a}{\tilde{n}} = \tilde{x}_r - \tilde{x}_{r-1}$ for all $r = 1, \dots, \tilde{n}$. The dimension of both spaces is $4n+2$, that is, the total number of interior knots is the same for both spaces, while the number of non-zero knot spans is different.

Moreover, we consider the two extended partitions $\mathbf{u}$, obtained by considering x_0 and x_n as knots of multiplicity four and adding two extra double knots outside the interval $[a,b]$ that we set to be

$$x_{-1} = x_0 - h \qquad \text{and} \qquad x_{n+1} = x_n + h,$$

and $\tilde{\mathbf{u}}$, obtained by extending the knot sequence of $\tilde{\mathbf{x}}$ by two sets of single knots as

$$\tilde{x}_{-k} = \tilde{x}_0 - k\tilde{h} \qquad \text{and} \qquad \tilde{x}_{\tilde{n}+k} = \tilde{x}_{\tilde{n}} + k\tilde{h}, \qquad k = 1, \dots, 5.$$

We define $\{\tilde{D}_k\}_{k=1}^{4n+2}$ the basis of the target space $S^{\tilde{n}}_{5,4}$ where

$$\tilde{D}_k(t) = [\tilde{x}_{k-6}, \dots, \tilde{x}_k](. - t)^5_+, \quad k = 1, \dots, 4n+2,$$

and we have that

$$I(\tilde{D}_k) = I(D_k), \qquad k = 6, \dots, 4n-3,$$

where $\{D_k\}_{k=1}^{4n+2}$ is the basis of the source space $S^n_{5,1}$, defined as in (2.6). The six boundary integrals (three only due to symmetry) are computed directly by integrating the corresponding B-splines. These integrals change during continuation and therefore have to be recomputed for various continuation parameter t, typically $t \in [0,1]$; $t=0$ (source), $t=1$ (target).

Now we consider a continuous transition between the source $S^n_{5,1}$ and target $S^{\tilde{n}}_{5,4}$. We set our source space as $S^n_{5,1}$ for which we know a Gaussian source quadrature rule of the form (2.7), with nodes and weights given in Theorem 2 and we look for a QR of the form

Table 1
Nodes and weights for Gaussian quadrature rules (2.11) for uniform knot distribution for various $\tilde{n}$. The integration interval is $[0, \frac{\tilde{n}+3}{4}]$ and thanks to symmetry properties only the first $\frac{\tilde{n}+3}{4}+1$ nodes and weights are reported.

i	τ_i	ω_i	$\|\mathbf{r}\|$	τ_i	ω_i	$\|\mathbf{r}\|$
	$\tilde{n}=9$		6.42(−18)	$\tilde{n}=13$		1.21(−17)
1	0.070809859159811	0.183349827808167		0.065385669153961	0.169325364763240	
2	0.377199653495331	0.423226004611632		0.348498904402831	0.391327681325333	
3	0.888400716916905	0.579969346497780		0.822112583828282	0.538918320717784	
4	1.500000000000000	0.626909642164842		1.395550612462171	0.596379706769487	
5	–	–		2.000000000000000	0.608097852848314	
	$\tilde{n}=17$		1.91(−17)	$\tilde{n}=21$		1.95(−17)
1	0.062501758846785	0.161857754107132		0.060716019702809	0.157233335577858	
2	0.333134377797970	0.374085047673794		0.323616604989813	0.363397640909352	
3	0.785911368439571	0.515262428552110		0.763459071760679	0.500544699204603	
4	1.334359996496279	0.570705014728738		1.296248210647031	0.554420719611212	
5	1.913781728943024	0.584630042082223		1.859170957103380	0.568041687847310	
6	2.500000000000000	0.586919425712005		2.428939359660305	0.570767137676093	
7	–	–		3.000000000000000	0.571189558347143	
	$\tilde{n}=25$		1.82(−17)	$\tilde{n}=29$		1.99(−17)
1	0.059501700174624	0.154088671891742		0.058622364733744	0.151811499504440	
2	0.317144284901381	0.356129713236112		0.312457423959895	0.350866713409836	
3	0.748189969221157	0.490533943462980		0.737132977306587	0.483284678101352	
4	1.270323682402073	0.543333040508792		1.251550440956447	0.535303513391059	
5	1.821989881285721	0.556684789756668		1.795064002776477	0.548458055855679	
6	2.380373136568870	0.559372890108410		2.345195639148952	0.551107018869507	
7	2.940067341931896	0.559878806579807		2.896620379924060	0.551608612579667	
8	3.500000000000000	0.559956288910975		3.448288240582612	0.551701856114277	
9	–	–		4.000000000000000	0.551716104348365	
	$\tilde{n}=33$		2.10(−17)	$\tilde{n}=37$		4.05(−17)
1	0.057956201499154	0.150086368831821		0.057434073557755	0.148734239383008	
2	0.308906771429059	0.346879591696191		0.306123827542799	0.343754550330581	
3	0.728756466293858	0.477792806922296		0.722191092726851	0.473488367225914	
4	1.237328277368729	0.529220519787704		1.226181175788537	0.524452767387078	
5	1.774665550962560	0.542225582588944		1.758677573121231	0.537340667590496	
6	2.318545703519458	0.544844463986058		2.297657904899482	0.539935956159231	
7	2.863704318670243	0.545340466255171		2.837905183402830	0.540427493680052	
8	3.409103572755148	0.545433231813783		3.378390942637572	0.540519443566724	
9	3.954547737362110	0.545450436137280		3.918921259881264	0.540536600406546	
10	4.500000000000000	0.545453063961504		4.459459881438810	0.540539780926602	
11	–	–		5.000000000000000	0.540540266687536	

$$\tilde{Q}_{2n+1}(f) = \sum_{i=1}^{2n+1} \tilde{\omega}_i f(\tilde{\tau}_i). \tag{2.11}$$

By using the homotopy framework, we are able to obtain the desired Gaussian QR. In Table 1 we report nodes and weights for various values of $\tilde{n}$. We also report the error $\|\mathbf{r}\|$ of the rule that is measured as the Euclidean norm of the vector of the residues, normalized by the system's dimension $4n+2=\tilde{n}+5$, i.e.,

$$\|\mathbf{r}\| = \frac{1}{\tilde{n}+5}\left(\sum_{i=1}^{\tilde{n}+5}(\tilde{Q}_{2n+1}(\tilde{D}_i) - I(\tilde{D}_i))^2\right)^{\frac{1}{2}}.$$

3. Numerical solution of linear Fredholm integral equations of the second kind via the Nyström method

Consider the linear Fredholm integral equation of the second kind

$$\lambda u(x) - \int_I k(x,y)\,u(y)\,dy = f(x), \quad x \in I := [a,b], \tag{3.1}$$

where $k(x,y)$ is a enough regular bivariate kernel.

Among the methods to solve (3.1) (see e.g. [3]), we are interested in the Nyström method. It stems in numerical integration of the integral operator in (3.1) using a numerical quadrature. To approximate the value of $I(g)$, we consider an m-point quadrature rule $Q_m(g)$ of kind (1.1), that is exact for some function space $\mathcal{L}$, i.e., $R_m(g)=0$ iff $g \in \mathcal{L}$. Traditionally, Gaussian quadrature for polynomials is used, i.e. $\mathcal{L}=\mathbb{P}_p$. The kernel k is assumed to be smooth, usually it is assumed to

be several times differentiable. The function g typically lies outside $\mathcal{L}$ and it is also assumed that there is a sequence of quadratures $(Q_m)_{m\geq 1}$ that converges to the exact integral as $m \to \infty$. Applying the quadrature rule to (3.1), one obtains

$$\lambda u_n(x) - \sum_{j=1}^{m} \omega_j k(x, \tau_j) u_n(\tau_j) = f(x), \quad x \in I, \tag{3.2}$$

where the unknown is the approximate solution u_n and the integer n is the number of elements, i.e., the uniform discretization of the interval I. Then the Nyström method proceeds by sampling x values at the quadrature points τ's also in the x-direction, which gives an $m \times m$ linear system

$$\lambda u_n(\tau_i) - \sum_{j=1}^{m} \omega_j k(\tau_i, \tau_j) u_n(\tau_j) = f(\tau_i), \quad i = 1, \ldots, m, \tag{3.3}$$

with the vector of unknowns

$$\mathbf{u}_n := (u_n(\tau_1), \ldots, u_n(\tau_m))^T.$$

Let $\mathbf{z} := (z_1, \ldots, z_m)^T$ be a solution of (3.3), then the solution reads as

$$z(x) = \frac{1}{\lambda}\left(f(x) + \sum_{j=1}^{m} \omega_j k(x, \tau_j) z_j \right),$$

which is known as *Nyström interpolation formula* [3].

Let us consider the Banach space $\mathcal{X} = C(I)$ and the operators $\mathcal{K}, \mathcal{K}_n : \mathcal{X} \to \mathcal{X}$ defined as

$$\mathcal{K}x(t) = \int_I k(t,s) x(s)\, ds \quad \text{and} \quad \mathcal{K}_n x(t) = \sum_{j=1}^{m} \omega_j k(t, \tau_j) x(\tau_j), \tag{3.4}$$

associated respectively with the integral equation (3.1) and a sequence of QRs

$$\int_a^b g(x)\, dx \approx \sum_{j=1}^{m} \omega_{n,j} g(\tau_{n,j}) \tag{3.5}$$

such that

$$\sup_{n\geq 1} \sum_{j=1}^{m} |\omega_{n,j}| < \infty.$$

To simplify the notation, we will omit the index n from now on.

It holds

$$\|\mathcal{K}_n\|_\infty = \max_{t\in I} \sum_{j=1}^{m} |\omega_j k(t, \tau_j)|.$$

With the notation given in (3.4), equations (3.1) and (3.2) read

$$(\lambda - \mathcal{K})u = f \quad \text{and} \quad (\lambda - \mathcal{K}_n)u_n = f.$$

Observe that m is the number of quadrature points and this number depends on n, the number of elements of the discretization, in various ways, depending on particular quadrature rules based on splines of various degrees and continuities or polynomial Gaussian ones. It holds that $m \to \infty$ as $n \to \infty$, but the concrete relation between m and n depends on the particular rule. For example, for the C^1 cubic spline space and its Gaussian quadrature we have $n = m + 1$, so asymptotically $n \approx m$. See later Table 3 in Section 4 for relations of m and n for other discretization spaces.

Next, we give a result on the convergence of the sequence $(u_n)_{n\geq 1}$ provided by the Nyström method when QRs for splines are used [3].

Theorem 3. *Let $k(t,x)$ be a continuous kernel defined on $D := I \times I$, and suppose that the sequence (3.5) of QRs converges for all continuous functions defined on I. Moreover, let us suppose that the integral equation (3.1) admits a unique solution for all function $f \in C(I)$ with $\lambda \neq 0$. Then, for n enough large, for instance $n \geq N$, the operator $(\lambda - \mathcal{K}_n)^{-1}$ exists and is uniformly bounded. More precisely, there exists a constant c_s such that*

Table 2
Seven test datasets for the Fredholm integral equations of the second kind. In turn, the columns contain the intervals, kernels, exact solutions, and right-handsides of (4.1).

i	I_i	$k_i(x,t)$	$u_i(x)$	$f_i(x)$
1	$[0,1]$	$\cos(\pi xt)$	e^{-x}	$e^{-x} - \frac{e+\pi x\sin(\pi x)-\cos(\pi x)}{(\pi^2x^2+1)e}$
2	$[0,1]$	e^{xt}	e^{x}	$e^{x} - \frac{e^{x+1}-1}{x+1}$
3	$[0,1]$	$\ln(1+x+t)$	$1-x+x^2-x^3$	$x\left(\frac{1}{4}x^3+\frac{4}{3}x^2+3x+4\right)\ln\left(\frac{x+1}{x+2}\right)$ $+\frac{25}{12}\ln(x+1)-\frac{8}{3}\ln(x+2)$ $-\frac{3}{4}x^3+\frac{47}{24}x^2+\frac{7}{12}x+\frac{385}{144}$
4	$[0,1]$	e^{xt}	$e^{-x}\cos x$	$e^{-x}\cos x - \frac{((x-1)\cos 1+\sin 1)e^{x}-e(x-1)}{e(x^2-2x+2)}$
5	$[0,\pi]$	$\cos(t+x)$	$\cos(50x)$	$\cos(50x) - \frac{2}{2499}\sin x$
6	$[0,\pi]$	e^{xt}	$x^2\cos(50x)$	$-\frac{1}{(2500+x^2)^3}\left(-2x\left(-7500+x^2\right)\right.$ $+e^{\pi x}\left(2x\left(-7500+x^2\right)+\pi^2x\left(2500+x^2\right)^2\right)$ $\left.+2\pi e^{\pi x}\left(6250000-x^4\right)\right)$ $+x^2\cos(50x)$
7	$[0,\pi]$	$t+x$	$e^{-x}\cos(50x)$	$-\frac{e^{-\pi}(2499-2501\pi-2501x+e^{\pi}(-2499+2501x))}{6255001}$ $+e^{-x}\cos(50x)$

$$\left\|(\lambda-\mathcal{K}_n)^{-1}\right\|_\infty \le \frac{1+\left\|(\lambda-\mathcal{K})^{-1}\right\|_\infty \|\mathcal{K}_n\|_\infty}{|\lambda|-\left\|(\lambda-\mathcal{K})^{-1}\right\|_\infty \|(\mathcal{K}-\mathcal{K}_n)\mathcal{K}_n\|_\infty} \le c_s,\ n\ge N.$$

Furthermore, for the solutions of equations $(\lambda-\mathcal{K})u=f$ *and* $(\lambda-\mathcal{K}_n)u_n=f$, $n\ge N$, *it holds*

$$\|u-u_n\|_\infty \le \left\|(\lambda-\mathcal{K}_n)^{-1}\right\|_\infty \|(\mathcal{K}-\mathcal{K}_n)u\|_\infty \le c_s\|(\mathcal{K}-\mathcal{K}_n)u\|_\infty .$$

We recall that the sequences of Gaussian QRs here considered are convergent for all continuous functions because they have positive weights (see e.g. [26, Theorem 3] and [12, p. 130]).

4. Numerical tests of the Nyström method based on QRs for splines

In this section, we consider seven integral equations

$$u_i(x) - \int_{a_i}^{b_i} k_i(x,t)\,u_i(t)\,dt = f_i(x),\ x\in I_i=[a_i,b_i], \tag{4.1}$$

whose kernels and independent terms are given in Table 2, as well as the corresponding solutions and the intervals I_i.

We numerically solve them by using the Nyström method in combination with the QRs proposed in Section 2 defined on a uniform partition of the interval I_i into n subintervals (elements). We compare the results with the ones produced when polynomial Gaussian quadratures are used. We develop all the tests in the Matlab environment.

The uniform norms $\|u_i-u_{i,n,\beta}\|_{\infty,I_i}$ of the errors $u_i-u_{i,n,\beta}$ between the exact and approximate solutions u_i and $u_{i,n,\beta}$ are estimated from their values at 1000 equispaced points in I_i, yielding values $e_{i,n,\beta}$. Here β denotes the QR applied in the Nyström method, in particular we use the following notation:

- $\beta=3$ for the QR exact on $S^n_{3,1}$;
- $\beta=5$ for the QR exact on $S^n_{5,1}$;
- $\beta=3H$ for the QR exact on $S^n_{3,2}$;
- $\beta=5H$ for the QR exact on $S^n_{5,4}$;
- $\beta=G2$ for the classical Gaussian rule with 2 nodes, exact on cubic polynomials;
- $\beta=G3$ for the classical Gaussian rule with 3 nodes, exact on quintic polynomials.

The numerical convergence orders are computed as

$$\mathcal{NCO}_\beta := \log_2 \frac{e_{i,n,\beta}}{e_{i,2n,\beta}}.$$

In order to qualitatively compare the results produced by different quadratures, we fix the number of nodes as this corresponds to the computational cost of the numerical integration. We consider the integers $m\in\{8,16,32,64,128\}$ and, for each fixed m, we compute the number of subintervals (aka elements) for each quadrature by using the relations reported in Table 3. In the case of spline Gaussian rules, the relation between m and n comes from the fact that the dimension of each corresponding spline space over n elements equals $2m$. The number of subintervals varies as it depends on the degree

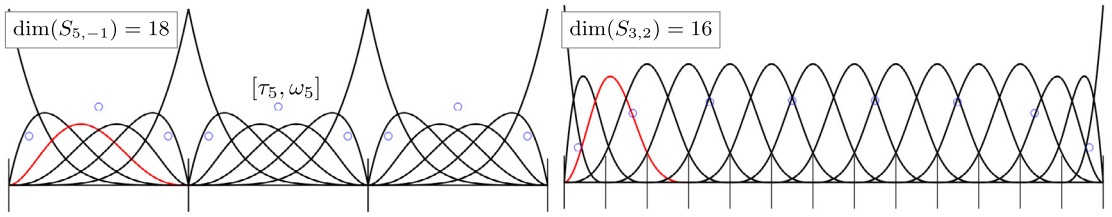

Fig. 2. Two spline spaces and their corresponding Gaussian quadratures used in the Nyström method. Left: Discontinuous (C^{-1}) quintic spline space over $n = 3$ elements and the corresponding polynomial Gauss quadrature (blue dots) applied elementwise with total $m = 9$ quadrature points. Right: C^2 cubic spline space over $n = 13$ uniform elements with its Gaussian quadrature consisting of only $m = 8$ quadrature points. (For interpretation of the colors in the figure(s), the reader is referred to the web version of this article.)

Table 3
Relation between the number of elements and number of nodes (middle column) and the number of elements (NoE) n (right) used for a fixed m to compare the results of the Nyström method using various quadrature rules (left), where $[\ell] := \text{round}(\ell)$.

	Relation between m and n	NoE
Formula exact in $S^n_{3,1}$	$m = n + 1$	$m - 1$
Formula exact in $S^n_{5,1}$	$m = 2n + 1$	$\left[\frac{m}{2}\right]$
Formula exact in $S^n_{3,2}$	$2m = n + 3$	$2m - 3$
Formula exact in $S^n_{5,4}$	$2m = n + 5$	$2m - 3$
Formula based on Q_2 [4]	$n = m$	m
Formula based on Q_4 [4]	$n = m$	m
Composite 2-nodes Gaussian Formula	$2n = m$	$\left[\frac{m}{2}\right]$
Composite 3-nodes Gaussian Formula	$3n = m$	$\left[\frac{m}{3}\right]$

Table 4
Results for example 1.

m	$n = m - 1$	$e_{1,n,3}$	$\mathcal{NCO}_3$	$n = \frac{m}{2}$	$e_{1,n,5}$	$\mathcal{NCO}_5$
8	7	2.13 (−05)	–	4	1.75 (−07)	–
16	15	1.04 (−06)	4.35	8	3.02 (−09)	5.85
32	31	5.70 (−08)	4.19	14	4.87 (−11)	5.95
64	63	3.33 (−09)	4.10	32	7.70 (−13)	5.98
128	127	2.01 (−10)	4.05	64	1.21 (−14)	5.99

m	$n = 2m - 3$	$e_{1,n,3H}$	$\mathcal{NCO}_{3H}$	$n = 2m - 3$	$e_{1,n,5H}$	$\mathcal{NCO}_{5H}$
8	13	1.49 (−06)	–	13	2.19 (−09)	–
16	29	6.43 (−08)	4.53	29	2.42 (−11)	6.50
32	61	3.31 (−09)	4.28	61	3.01 (−13)	6.33
64	125	1.88 (−10)	4.14	125	4.22 (−15)	6.16
128	253	1.12 (−11)	4.07	253	7.77 (−16)	2.44

and continuity of the underlying spline space. In cases where the particular number of nodes does not permit admissible number of elements (i.e., n is not integer in Table 3) or it does not permit to satisfy the relations explained in Section 2.4, we round n up to fairly compare spline spaces with (almost) the same dimension, and consequently almost the same number of nodes. This is depicted in Fig. 2 where two spline space requiring almost the same number of quadrature points are shown. Observe a lot higher flexibility of the spline space that spans $n = 13$ elements while the discontinuous counterpart spans only $n = 3$ elements, yet being of even a slightly higher dimension. This phenomenon is reflected by larger approximation error when using standard polynomial Gaussian quadrature in contrast to some spline alternatives.

Tables 4 and 8 contain estimations of the errors provided by the different methods used to compute numerical solutions to the first integral equation whose kernel, independent term and exact solution are given in Table 2.

These results confirm the theoretical ones regarding the numerical convergence orders. They are equal to 4 for the formulas based on cubic splines and 6 for the formulas based on quintic splines. Comparing formulas with the same convergence order, we can conclude that the QRs constructed in Section 2.4 produce better results.

When compared to polynomial Gaussian quadrature, the Gaussian quadratures for splines exploit the continuity between the polynomial pieces and therefore would not capture behavior of a function with low continuity. If, for example, the right hand-side of (3.1) is discontinuous, it is not recommended to use spline quadratures as they might underintegrate the solution.

The conclusions are similar for the other examples, whose results are given in Tables 5-11. Observe that when we do not have results of errors for certain values of m in these tables, it is because the double float precision of our Matlab implementation was reached.

Table 5
Results for example 2.

m	$n=m-1$	$e_{2,n,3}$	$\mathcal{NCO}_3$	$n=\frac{m}{2}$	$e_{2,n,5}$	$\mathcal{NCO}_5$
8	7	2.59(−05)	–	4	5.63(−08)	–
16	15	1.40(−06)	4.21	8	1.03(−09)	5.77
32	31	8.16(−08)	4.11	14	1.74(−11)	5.89
64	63	4.92(−09)	4.05	32	2.83(−13)	5.94
128	127	3.02(−10)	4.03	64	1.51(−14)	4.23
m	$n=2m-3$	$e_{2,n,3H}$	$\mathcal{NCO}_{3H}$	$n=2m-3$	$e_{2,n,5H}$	$\mathcal{NCO}_{5H}$
	$2m-3$			$2m-3$		
8	13	2.01(−06)	–	13	1.28(−10)	–
16	29	9.02(−08)	4.48	29	6.00(−12)	5.95
32	61	4.82(−09)	4.22	61	5.31(−13)	6.10
64	125	2.79(−10)	4.11	125	1.10(−15)	4.39
128	253	1.68(−11)	4.05	253	–	–

Table 6
Results for example 3.

m	$n=m-1$	$e_{3,n,3}$	$\mathcal{NCO}_3$	$n=\frac{m}{2}$	$e_{3,n,5}$	$\mathcal{NCO}_5$
8	7	2.22 (−05)	–	4	5.29 (−08)	–
16	15	1.20 (−06)	4.21	8	1.02 (−09)	5.70
32	31	6.96 (−08)	4.11	14	1.78 (−11)	5.84
64	63	4.19 (−09)	4.05	32	2.96 (−13)	5.91
128	127	2.57 (−10)	4.03	64	8.77 (−15)	5.08
m	$n=2m-3$	$e_{3,n,3H}$	$\mathcal{NCO}_{3H}$	$n=2m-3$	$e_{3,n,5H}$	$\mathcal{NCO}_{5H}$
8	13	1.72 (−06)	–	13	1.29 (−10)	–
16	29	7.69 (−08)	4.48	29	6.31 (−12)	5.21
32	61	4.11 (−09)	4.23	61	5.70 (−14)	5.91
64	125	2.38 (−10)	4.11	125	1.18 (−15)	–
128	253	1.43 (−11)	4.05	253	–	–

Table 7
Results for example 4.

m	$n=m-1$	$e_{4,n,3}$	$\mathcal{NCO}_3$	$n=\frac{m}{2}$	$e_{4,n,5}$	$\mathcal{NCO}_5$
8	7	1.91 (−06)	–	4	1.01 (−09)	–
16	15	1.01 (−07)	4.24	8	1.80 (−11)	5.81
32	31	5.82 (−09)	4.12	14	2.98 (−13)	5.92
64	63	3.48 (−10)	4.06	32	5.47 (−15)	5.77
128	127	2.13 (−11)	4.03	64	–	–
m	$n=2m-3$	$e_{4,n,3H}$	$\mathcal{NCO}_{3H}$	$n=2m-3$	$e_{4,n,5H}$	$\mathcal{NCO}_{5H}$
8	13	1.45 (−07)	–	13	9.92 (−12)	–
16	29	6.45 (−09)	4.49	29	1.32 (−13)	6.23
32	61	3.42 (−10)	4.24	61	2.36 (−15)	5.81
64	125	1.97 (−11)	4.11	125	–	–
128	253	1.18 (−12)	4.06	253	–	–

In the last three examples, solution functions $u_i(x)$ are highly oscillating functions. Observe that the performances of the QRs in Section 2.4 are by several orders of magnitude better when compared to their polynomial Gauss counterparts. Note that, due to the oscillatory behavior of $u_i(x)$, the error is large for small number of elements and therefore we start with $n=32$ and $n=16$ in Table 10 and 11, respectively.

5. Numerical solution of Hammerstein integral equations via the Nyström method

In this section we consider Hammerstein integral equations of the form

$$u(x)-\int_I k(x,y)g(y,u(y))dy=f(x),\qquad x\in I:=[a,b], \tag{5.1}$$

where the kernel $k(x,y)$ and the function $f(x)$ are given, and $g(x,u(x))$ is a non-linear function of $u(x)$ while the unknown function $u(x)$ represents the solution of the integral equation. The existence and the uniqueness of solutions to this type of

Table 8
From top to bottom and from left to right, results for examples 1, 2, 3 and 4 using classical Gaussian rules with 2 and 3 nodes.

m	$e_{1,n,G2}$ $n=\frac{m}{2}$	$e_{1,n,G3}$ $n=\left\lceil\frac{m}{3}\right\rceil$	$e_{2,n,G2}$ $n=\frac{m}{2}$	$e_{2,n,G3}$ $n=\left\lceil\frac{m}{3}\right\rceil$
8	3.49 (−05)	3.55 (−07)	5.14 (−05)	1.28 (−07)
16	2.14 (−06)	1.62 (−08)	3.23 (−06)	6.00 (−09)
32	1.33 (−07)	1.41 (−10)	2.02 (−07)	5.31 (−11)
64	8.30 (−09)	2.91 (−12))	1.26 (−08)	1.10 (−12)
128	5.19 (−10)	3.95 (−14)	7.90 (−10)	1.87 (−14)
m	$e_{3,n,G2}$ $n=\frac{m}{2}$	$e_{3,n,G3}$ $n=\left\lceil\frac{m}{3}\right\rceil$	$e_{4,n,G2}$ $n=\frac{m}{2}$	$e_{4,n,G3}$ $n=\left\lceil\frac{m}{3}\right\rceil$
8	4.38 (−05)	1.29 (−07)	3.65 (−06)	2.19 (−09)
16	2.75 (−06)	6.31 (−09)	2.28 (−07)	1.01 (−10)
32	1.72 (−07)	5.70 (−11)	1.42 (−08)	8.94 (−13)
64	1.08 (−08)	1.18 (−12)	8.89 (−10)	1.87 (−14)
128	6.73 (−10)	1.68 (−14)	5.56 (−11)	9.16 (−16)

Table 9
Results for example 5.

m	$e_{5,n,3}$ $n=m-1$	$e_{5,n,5}$ $n=\frac{m}{2}$	$e_{5,n,3H}$ $n=2m-3$	$e_{5,n,5H}$ $n=2m-3$	$e_{5,n,G2}$ $n=\frac{m}{2}$	$e_{5,n,G3}$ $n=\left\lceil\frac{m}{3}\right\rceil$
8	5.39 (−02)	5.04 (−01)	2.57 (−01)	9.00 (−02)	4.37 (−02)	2.37 (−01)
16	4.83 (−03)	2.04 (−02)	4.66 (−03)	5.04 (−03)	1.72 (−01)	7.44 (−01)
32	4.46 (−03)	9.84 (−05)	2.55 (−03)	3.70 (−03)	3.11 (−03)	9.30 (−03)
64	2.01 (−05)	1.43 (−04)	9.54 (−06)	2.17 (−08)	8.28 (−04)	4.87 (−05)
128	1.17 (−06)	5.56 (−08)	9.43 (−08)	3.15 (−11)	1.10 (−05)	3.93 (−06)

Table 10
Results for example 6.

m	$e_{6,n,3}$ $n=m-1$	$e_{6,n,5}$ $n=\frac{m}{2}$	$e_{6,n,3H}$ $n=2m-3$	$e_{6,n,5H}$ $n=2m-3$	$e_{6,n,G2}$ $n=\frac{m}{2}$	$e_{6,n,G3}$ $n=\left\lceil\frac{m}{3}\right\rceil$
32	7.80 (+00)	6.61 (+00)	1.61 (+00)	8.07 (−01)	1.04 (+01)	3.56 (+00)
64	9.94 (−02)	3.29 (−01)	2.54 (−02)	5.46 (−04)	2.52 (+00)	3.56 (−01)
128	1.43 (−02)	1.11 (−03)	6.10 (−04)	6.93 (−06)	4.43 (−02)	1.43 (−02)

Table 11
Results for example 7.

m	$e_{7,n,3}$ $n=m-1$	$e_{7,n,5}$ $n=\frac{m}{2}$	$e_{7,n,3H}$ $n=2m-3$	$e_{7,n,5H}$ $n=2m-3$	$e_{7,n,G2}$ $n=\frac{m}{2}$	$e_{7,n,G3}$ $n=\left\lceil\frac{m}{3}\right\rceil$
16	8.05 (−02)	5.20 (−02)	4.04 (−02)	7.69 (−02)	9.86 (−02)	3.75 (−01)
32	8.21 (−03)	1.03 (−02)	1.68 (−02)	5.78 (−03)	3.30 (−03)	9.15 (−03)
64	3.38 (−04)	1.40 (−04)	2.21 (−05)	5.66 (−06)	8.76 (−04)	4.15 (−05)
128	2.60 (−05)	2.12 (−06)	4.77 (−07)	2.80 (−08)	1.18 (−05)	4.19 (−06)

integral equations have been investigated in the literature by many authors (see e.g. [28]). Hammerstein integral equations arise in several applications in physics and engineering, such as in fluid mechanics, biological models, solid state physics, kinetics in chemistry, etc. In most cases, it is difficult to solve them, especially analytically.

For $g \in \mathcal{C}(I)$, the integral operator can be approximated in the following way

$$\int_I k(x,y)g(y,u(y))dy \approx \sum_{j=1}^{m} \omega_j k\left(x,\tau_j\right) g\left(\tau_j, u_n\left(\tau_j\right)\right),$$

where ω_j e τ_j are weights and nodes of the QR, respectively. Thus, we approximate integral equation (5.1) by

$$u_n(x) - \sum_{j=1}^{m} \omega_j k\left(x,\tau_j\right) g\left(\tau_j, u_n\left(\tau_j\right)\right) = f(x), \quad x \in I. \tag{5.2}$$

This is equivalent to first solve the system of non-linear equations

Table 12
Three test datasets for the Hammerstein integral equations.

i	$k_i(x,t)$	$g_i(t,u)$	$u_i(x)$	$f_i(x)$
1	$\cos(\pi x)\sin(\pi t)$	u^2	$\sin(\pi x)$	$\sin(\pi x) - \frac{4}{3\pi}\cos(\pi x)$
2	$-x$	e^u	x	e^x
3	$-e^{x-2t}$	u^3	e^x	e^{x+1}

$$u_n(\tau_i) - \sum_{j=1}^{m} \omega_j k\left(\tau_i, \tau_j\right) g\left(\tau_j, u_n\left(\tau_j\right)\right) = f(\tau_i), \quad i = 1, \ldots, m,$$

where the unknowns are the values $u_n(\tau_i)$, $1 \le i \le m$ and then obtain the approximate solution by (5.2)

$$u_n(x) = \left(f(x) + \sum_{j=1}^{m} \omega_j k\left(x, \tau_j\right) g\left(\tau_j, u_n\left(\tau_j\right)\right) \right).$$

Let us consider the Banach space $\mathcal{X} = C(I)$ and the non-linear operators $\mathcal{K}, \mathcal{K}_n : \mathcal{X} \to \mathcal{X}$ defined as

$$\mathcal{K}x(t) = \int_I k(t,s) g(s, x(s)) ds,$$

$$\mathcal{K}_n x(t) = \sum_{j=1}^{m} \omega_j k(t, \tau_j) g(\tau_j, x(\tau_j)), \qquad t \in I, \qquad x \in \mathcal{C}(I).$$

Moreover, we assume that the following assumptions are satisfied [2]:

1. $\mathcal{K}$ and $\mathcal{K}_n$, $n \ge 1$, are completely continuous operators on Ω into $\mathcal{X}$, where Ω is an open connected subset of $\mathcal{X}$;
2. $\{\mathcal{K}_n\}_{n\ge1}$ is a collectively compact family on Ω;
3. $\mathcal{K}_n \to \mathcal{K}$ as $n \to \infty$, all $x \in \Omega$;
4. $\{\mathcal{K}_n\}_{n\ge1}$ is equicontinuous at each $x \in \Omega$.

We also assume that the integral equation (5.1) has a unique solution for $f \in \mathcal{C}(I)$ and we denote the solution by x_*. In order to compute the convergence rate, assume $[I - \mathcal{K}'(x_*)]^{-1}$ exists on $\mathcal{X}$, where $\mathcal{K}'(x_*)$ denotes the Fréchet derivative of $\mathcal{K}(x)$ in x_* and further assume

$$\|\mathcal{K}_n'(x)\| \le c_1 < \infty, \quad \|\mathcal{K}_n''(x)\| \le c_2 < \infty$$

for $n \ge 1$ and $\|x_* - x_n\| \le \varepsilon$, with ε, c_1 e $c_2 > 0$. Then [2]

$$\|x_* - x_n\| \le c\|\mathcal{K}(x_*) - \mathcal{K}_n(x_*)\|, \qquad n \ge N.$$

Thus, the speed of convergence is that of the numerical integration method applied to $\mathcal{K}(x_*)$, and this is usually obtained easily.

5.1. Numerical tests

In this section, we consider three integral equations

$$u_i(x) - \int_0^1 k_i(x,t)\, g_i(t, u_i(t))\, dt = f_i(x), \; x \in [0,1],$$

whose corresponding data are given in Table 12.

We numerically solve them by using the Nyström method in combination with the QRs proposed in Section 2 defined on a uniform partition of the interval $[0,1]$ into n subintervals. We compare the results with the ones produced when polynomial Gaussian quadratures are used and with those obtained in [5]. We develop all the tests in the Matlab environment. For the solution of the non-linear systems we use the `fsolve` command.

The uniform norms $\|u_i - u_{i,n,\beta}\|_{\infty,[0,1]}$ of the errors $u_i - u_{i,n,\beta}$ between the exact and approximate solutions u_i and $u_{i,n,\beta}$ are estimated from their values at 1000 equispaced points in $[0,1]$, yielding values $e_{i,n,\beta}$. As in Section 4, β denotes the QR applied in the Nyström method. Moreover, here we consider

- $\beta = 3nu$ for the QR based on the non-uniform quadratic quasi-interpolant Q_3, as explained in [5]. The formula is of order $O\left(h^4\right)$;

Table 13
Results for example 1 – non-linear case.

m	$n=m-1$	$e_{1,n,3}$	$\mathcal{NCO}_3$	$n=\frac{m}{2}$	$e_{1,n,5}$	$\mathcal{NCO}_5$
8	7	1.07 (−04)	–	4	4.27 (−06)	–
16	15	8.93 (−06)	3.59	8	1.77 (−07)	4.60
32	31	5.43 (−07)	4.04	14	3.39 (−09)	5.70
64	63	3.26 (−08)	4.06	32	5.56 (−11)	5.93
128	127	1.98 (−09)	4.04	64	8.80 (−13)	5.98
m	$n=2m-3$	$e_{1,n,3H}$	$\mathcal{NCO}_{3H}$	$n=2m-3$	$e_{1,n,5H}$	$\mathcal{NCO}_{5H}$
8	13	9.27 (−06)	–	13	1.30 (−08)	–
16	29	5.33 (−07)	4.11	29	1.08 (−09)	3.59
32	61	3.13 (−08)	4.09	61	2.00 (−11)	5.75
64	125	1.83 (−09)	4.09	125	2.99 (−13)	6.06
128	253	1.10 (−10)	4.06	253	4.75 (−15)	5.98

Table 14
Results for example 1 – non-linear case.

m	$e_{1,n,3nu}$ $n=m$	$e_{1,n,5nu}$ $n=m$	$e_{1,n,G2}$ $n=\frac{m}{2}$	$e_{1,n,G3}$ $n=\left[\frac{m}{3}\right]$
8	1.38 (−04)	1.36 (−03)	4.14 (−04)	3.65 (−05)
16	7.99 (−06)	2.86 (−05)	2.21 (−05)	1.32 (−06)
32	4.94 (−07)	4.79 (−07)	1.33 (−06)	1.05 (−08)
64	3.08 (−08)	7.61 (−09)	8.24 (−08)	2.14 (−10))
128	1.93 (−09)	1.49 (−10)	5.14 (−09)	2.88 (−12)

Table 15
Results for example 2 – non-linear case.

m	$n=m-1$	$e_{2,n,3}$	$\mathcal{NCO}_3$	$n=\frac{m}{2}$	$e_{2,n,5}$	$\mathcal{NCO}_5$
8	7	3.99 (−07)	–	4	2.62 (−10)	–
16	15	2.14 (−08)	4.22	8	4.74 (−12)	5.79
32	31	1.23 (−09)	4.12	14	7.23 (−14)	6.04
64	63	7.41 (−11)	4.06	32	2.66 (−15)	4.76
128	127	4.54 (−12)	4.03	64	–	–
m	$n=2m-3$	$e_{2,n,3H}$	$\mathcal{NCO}_{3H}$	$n=2m-3$	$e_{2,n,5H}$	$\mathcal{NCO}_{5H}$
8	13	3.06 (−08)	–	13	2.27 (−12)	–
16	29	1.37 (−09)	4.49	29	3.30 (−14)	3.59
32	61	7.27 (−11)	4.23	61	–	–
64	125	4.20 (−12)	4.11	125	–	–
128	253	2.53 (−13)	4.06	253	–	–

Table 16
Results for example 2 – non-linear case.

m	$e_{2,n,3nu}$ $n=m$	$e_{2,n,5nu}$ $n=m$	$e_{2,n,G2}$ $n=\frac{m}{2}$	$e_{2,n,G3}$ $n=\left[\frac{m}{3}\right]$
8	3.41 (−07)	2.17 (−07)	7.75 (−07)	5.82 (−10)
16	2.18 (−08)	5.31 (−10)	4.85 (−08)	2.72 (−11)
32	1.36 (−09)	9.24 (−12)	3.03 (−09)	2.27 (−13)
64	8.46 (−11)	1.49 (−13)	1.90 (−10)	6.22 (−15))
128	5.29 (−12)	2.89 (−15)	1.19 (−11)	–

- $\beta = 5nu$ for the QR based on the non-uniform quartic quasi-interpolant Q_5, as explained in [5]. The formula is of order $O\left(h^6\right)$.

As in Section 4, we consider the integers $m \in \{8, 16, 32, 64, 128\}$ and for each on them we compute the number of subintervals for each quadrature by using the relations reported in Table 3.

Tables 13-18 contain estimations of the errors provided by the different methods used to compute numerical solutions of the three integral equations (when we do not have results of errors for certain values of m in these tables, it is because the double float precision of our Matlab implementation was reached).

These results confirm the theoretical ones regarding the numerical convergence orders. They are equal to 4 for the formulas based on cubic splines and 6 for the formulas based on quintic splines. Comparing formulas with the same convergence order, we conclude that, among the quadrature rules tested, the spline Gaussian rules with maximum continuity, described

Table 17
Results for example 3 – non-linear case.

m	$n=m-1$	$e_{3,n,3}$	$\mathcal{NCO}_3$	$n=\frac{m}{2}$	$e_{3,n,5}$	$\mathcal{NCO}_5$
8	7	3.53 (−07)	–	4	2.31 (−10)	–
16	15	1.89 (−08)	4.22	8	4.19 (−12)	5.79
32	31	1.09 (−09)	4.12	14	7.11 (−14)	5.88
64	63	6.54 (−11)	4.06	32	4.00 (−15)	4.15
128	127	4.01 (−12)	4.03	64	–	–

m	$n=2m-3$	$e_{3,n,3H}$	$\mathcal{NCO}_{3H}$	$n=2m-3$	$e_{3,n,5H}$	$\mathcal{NCO}_{5H}$
8	13	2.70 (−08)	–	13	2.01 (−12)	–
16	29	1.21 (−09)	4.49	29	3.11 (−14)	6.01
32	61	6.42 (−11)	4.23	61	2.66 (−15)	3.54
64	125	3.71 (−12)	4.11	125	–	–
128	253	2.260 (−13)	4.04	253	–	–

Table 18
Results for example 3 – non-linear case.

m	$e_{3,n,3nu}$ $n=m$	$e_{3,n,5nu}$ $n=m$	$e_{3,n,G2}$ $n=\frac{m}{2}$	$e_{3,n,G3}$ $n=\left[\frac{m}{3}\right]$
8	3.01 (−07)	1.92 (−08)	6.85 (−07)	5.14 (−10)
16	1.92 (−08)	4.69 (−10)	4.29 (−08)	2.41 (−11)
32	1.20 (−09)	8.16 (−12)	2.68 (−09)	2.12 (−13)
64	7.48 (−11)	1.30 (−13)	1.68 (−10)	7.99 (−15))
128	4.67 (−12)	3.55 (−15)	1.05 (−11)	–

in Section 2.4, produce the best solutions. In particular, when compared to the classical polynomial Gauss quadrature, the approximated solutions are by two to three orders of magnitude better.

6. Conclusions

We solve Fredholm linear integral equations of the second kind and non-linear Hammerstein integral equations via Nyström method using various existing spline Gaussian quadrature rules and newly derived rules for quintic C^4 spline spaces with uniform knots. We prove that the method converges to the exact solution as the number of uniformly distributed elements goes to infinity and show numerically that, in the majority of the test cases, using spline Gaussian rules the approximation error is smaller by several orders of magnitude than the one when the classical polynomial Gaussian rule is used.

Acknowledgements

The first author acknowledges partial financial support by the IMAG–María de Maeztu grant CEX2020-001105-M / AEI / 10.13039/501100011033. The second author has been partially supported by Spanish State Research Agency (Spanish Ministry of Science, Innovation and Universities): BCAM Severo Ochoa excellence accreditation SEV-2017-0718 and by Ramón y Cajal with reference RYC-2017-22649. The fourth author is member of GNCS-INdAM.

References

[1] R. Ait-Haddou, M. Bartoň, V.M. Calo, Explicit Gaussian quadrature rules for C^1 cubic splines with symmetrically stretched knot sequences, J. Comput. Appl. Math. 290 (2015) 543–553.
[2] K.E. Atkinson, A survey of numerical methods for solving nonlinear integral equations, J. Integral Equ. Appl. 4 (1992) 15–46.
[3] K.E. Atkinson, The Numerical Solution of Integral Equations of the Second Kind, Cambridge University Press, Cambridge, 1997.
[4] D. Barrera, F. Elmokhtari, D. Sbibih, Two methods based on bivariate spline quasi-interpolants for solving Fredholm integral equations, Appl. Numer. Math. 127 (2018) 78–94.
[5] D. Barrera, F. El Mokhtari, M.J. Ibáñez, D. Sbibih, Non-uniform quasi-interpolation for solving Hammerstein integral equations, Int. J. Comput. Math. 97 (2020) 72–84.
[6] M. Bartoň, V.M. Calo, Gaussian quadrature for splines via homotopy continuation: rules for C^2 cubic splines, J. Comput. Appl. Math. 296 (2016) 709–723.
[7] M. Bartoň, V.M. Calo, Optimal quadrature rules for odd-degree spline spaces and their application to tensor-product-based isogeometric analysis, Comput. Methods Appl. Mech. Eng. 305 (2016) 217–240.
[8] M. Bartoň, V.M. Calo, Gauss-Galerkin quadrature rules for quadratic and cubic spline spaces and their application to isogeometric analysis, Comput. Aided Des. 82 (2017) 57–67.
[9] M. Bartoň, R. Ait-Haddou, V.M. Calo, Gaussian quadrature rules for C^1 quintic splines with uniform knot vectors, J. Comput. Appl. Math. 322 (2017) 57–70.
[10] C. Dagnino, S. Remogna, P. Sablonnière, On the solution of Fredholm integral equations based on spline quasi-interpolating projectors, BIT Numer. Math. 54 (2014) 979–1008.

[11] C. Dagnino, A. Dallefrate, S. Remogna, Spline quasi-interpolating projectors for the solution of nonlinear integral equations, J. Comput. Appl. Math. 354 (2019) 360–372.
[12] P.J. Davis, P. Rabinowitz, Methods of Numerical Integration, second edition, Computer Science and Applied Mathematics, Academic Press, Inc., Orlando, FL, 1984.
[13] C. de Boor, A Practical Guide to Splines, revised edition, Springer, New York, 2001.
[14] W. Gautschi, Numerical Analysis, Springer, 1997.
[15] G.H. Golub, J.H. Welsch, Calculation of Gauss quadrature rules, Math. Comput. 23 (1969) 221–230.
[16] T.J. Hughes, A. Reali, G. Sangalli, Efficient quadrature for NURBS-based isogeometric analysis, Comput. Methods Appl. Mech. Eng. 199 (5–8) (2010) 301–313.
[17] S. Karlin, W.J. Studden, Tchebyscheff Systems: with Applications in Analysis and Statistics, Interscience Publications, New York, 1966.
[18] C.A. Micchelli, The fundamental theorem of algebra for monosplines with multiplicities, in: Lineare Oper. Approx., 1972, pp. 419–430.
[19] C.A. Micchelli, A. Pinkus, Moment theory for weak Chebyshev systems with applications to monosplines, quadrature formulae and best one-sided l^1 approximation by spline functions with fixed knots, SIAM J. Math. Anal. 8 (1977) 206–230.
[20] F. Mirzaee, Using rationalized Haar wavelet for solving linear integral equations, Appl. Math. Comput. 160 (2005) 579–587.
[21] F. Mirzaee, E. Hadadiyan, Numerical solution of linear Fredholm integral equations via two-dimensional modification of hat functions, Appl. Math. Comput. 280 (2015) 805–816.
[22] F. Mirzaee, E. Hadadiyan, Numerical solution of Volterra–Fredholm integral equations via modification of hat functions, Appl. Math. Comput. 280 (2016) 110–123.
[23] F. Mirzaee, S.F. Hoseini, Application of Fibonacci collocation method for solving Volterra–Fredholm integral equations, Appl. Math. Comput. 273 (2016) 637–644.
[24] G. Nikolov, On certain definite quadrature formulae, J. Comput. Appl. Math. 75 (1996) 329–343.
[25] L. Pretorius, D. Eyre, Spline-Gauss rules and the Nyström method for solving integral equations in quantum scattering, J. Comput. Appl. Math. 18 (1987) 235–247.
[26] I.J. Schoenberg, Spline functions, convex curves and mechanical quadrature, Bull. Am. Math. Soc. 64 (1958) 352–357.
[27] C.W. Wampler, A.J. Sommese, The Numerical Solution of Systems of Polynomials Arising in Engineering and Science, World Scientific, Singapore, 2005.
[28] A.M. Wazwaz, Linear and Nonlinear Integral Equations: Methods and Applications, Springer, Berlin, 2011.